

Apple Pectic Gel Produced by Dehydration

Evangelina Leiva Díaz · Leda Giannuzzi · Sergio A. Giner

Received: 5 September 2007 / Accepted: 31 October 2007 / Published online: 4 December 2007
© Springer Science + Business Media, LLC 2007

Abstract A novel, flexible sheet-like food formed by the high methoxyl pectin–sugar–acid gelation during drying of apple puree was investigated to characterize drying-related properties. Product volume was reduced by 68% over the process, and this shrinkage was successfully modeled by assuming the volume reduction equal to the volume of water evaporated. The sorption isotherm at 25 °C was determined, and a new expression for the moisture content, W , as a function of water activity, a_w , of the type $W = C_1 \exp(C_2 a_w^{C_3})$ resulted as the most accurate for this J-shaped isotherm. The drying kinetics was studied at 50, 60, and 80 °C in a tray dryer. No constant drying rate period was found, and the drying curve was divided in high- and low-moisture zones. For high moistures, an internal–external mixed control diffusive model coupling mass and heat transfer was applied to obtain a mass transfer

Biot number of 2.1. In the low-moisture zone, a diffusive, isothermal drying model for strict internal control was utilized. Diffusivities varied around 1×10^{-9} m²/s for high moistures and were about ten times lower at low moistures, although the activation energies were comparable (15,259 and 16,800 J/mol, respectively). The drying time at 60 °C was 6.67 h. The product scored four points out of five in a sensory evaluation of general acceptability.

Keywords Fruit leather · Hot-air drying · Non-isothermal drying

Nomenclature

A	mass transfer area for evaporation (m ²)
a_w	water activity, decimal
A_h and B_h	fitting parameters of the Halsey model
A_o and B_o	fitting parameters of the Oswin model
$a, b, c,$ and d	coefficients of the third degree polynomials $W=f(t)$
Bi	mass transfer Biot number
C_p	specific heat of apples (J kg ⁻¹ K ⁻¹)
C	constant of the GAB model
C_1, C_2, C_3	parameters of the new sorption model
D	effective diffusion coefficient of water (m ² /s)
d	average laminate thickness (m)
D_0	Arrhenius preexponential factor (m ² /s)
E_a	activation energy (J/mol)
f	multiplier of the preliminary Arrhenius preexponential factor
h	heat transfer coefficient (W/°C m ²)
h_a	air absolute humidity (kg vapor/kg dry air)
h_r	air relative humidity (decimal)
k	constant of the GAB model
L_{wd}	product heat of desorption (J/kg)

E. Leiva Díaz · L. Giannuzzi · S. A. Giner (✉)
Centro de Investigación y Desarrollo en Criotecología
de Alimentos (CIDCA), CONICET,
Universidad Nacional de La Plata (UNLP),
Calle 47 y 116,
B1900 AJJ La Plata, Argentina
e-mail: saginer@ing.unlp.edu.ar

E. Leiva Díaz · S. A. Giner
Facultad de Ingeniería, UNLP,
47 y 116,
La Plata 1900, Argentina

S. A. Giner
Comisión de Investigaciones Científicas de la Provincia
de Buenos Aires,
Buenos Aires, Argentina

E. Leiva Díaz · L. Giannuzzi
CONICET, Consejo Nacional de Investigaciones
Científicas y Técnicas,
Buenos Aires, Argentina

L_w	heat of vaporization of water (J/kg)
m	product mass at any time (kg)
m_0	initial product mass (kg)
m_d	product dry matter (kg)
m_{wev}	mass of water evaporated (kg)
MSS	sum of squares of the deviation
M_{1n}, M_{2n}, M_{3n} and M_{4n}	values of parameters of Eq. 15
r^2	coefficient of determination
R	universal gas constant $8.314 \text{ J mol}^{-1} \text{ K}^{-1}$
t	time (s)
T_a	air temperature ($^{\circ}\text{C}$)
T_0	product temperature at $t=0$ ($^{\circ}\text{C}$)
T	product temperature ($^{\circ}\text{C}$)
V	product volume at W (m^3)
V_0	initial product volume (m^3)
V_d	dry matter volume (m^3)
V_{wev}	volume of water evaporated (m^3)
W	moisture content (dec., d.b.)
\bar{W}	product average moisture content (dec., d.b.)
W_e	equilibrium moisture content (dec., d.b.)
W_0	initial moisture content (dec., d.b.)
W_m	monolayer moisture content of the GAB model (dec., d.b.)
W_{ad}	dimensionless moisture content
β_n	roots of the equation $\beta_n \tan \beta_n - \text{Bi} = 0$
ρ	product density (kg/m^3)
ρ_d	dry matter density (kg/m^3)
ρ_w	liquid water density (kg/m^3)
<i>Subscripts</i>	
hm	high-moisture zone
lm	low-moisture zone

Introduction

The hot air drying of fruits has been studied mainly as a preservation method for cut, peeled tissue pieces (Copley and Van Arsdel 1973; Barbosa-Cánovas and Vega-Mercado 1996; Greensmith 1998). However, their quality parameters are usually unsatisfactory when compared to the fresh because of shape deformation, membrane cell rupture, and incomplete rehydration. Krokida and Marinos-Kouris (2003) studied the rehydration capacity of several dried products and concluded that higher rehydration temperatures lead to higher water uptake by the product. This, in principle, is a good feature, but higher temperatures can adversely affect nutritional properties and organoleptic parameters of the product and may leave valuable minerals and water soluble vitamins in the rehydration medium.

Dryer design requires a model consisting of a set of four differential equations describing the variation of moisture

and temperature in product and air, as a function of position and time (Crapiste and Rotstein 1997). The main components of such models are the drying kinetic expressions describing the average product moisture content and temperature as a function of time. In some contributions, empirical models are developed to predict only the variation of moisture content (Krokida et al. 2004); these models are useful for quick-drying time estimations but do not identify the drying mechanism and cannot be used to estimate quality losses. In contrast, some models have been developed for cellular foods, which are important to provide basic knowledge for drying science (Crapiste et al. 1988a, b). Their application, however, requires numerous coefficients to simulate the process whose determination methods were not yet devised.

From the reviews by Mulet (1994) and Ratti (2001), it becomes evident that well-founded models yet of manageable complexity are required to predict the coupled drying and heating rates to enable the prediction of drying curves, drying times, and eventually, quality losses. These models should also be able to provide some insight into the drying mechanism.

Roques (2005) identified research needs on new dried materials and new drying techniques. In this regard, Wolf et al. (1990) reported “fruit leathers” (notably apple) as novel products made by pureeing fresh fruits followed by hot-air dehydration to form a flexible, sweet product. As they are processed products to be consumed as low-moisture foods, their quality index cannot be represented by the rehydration test. Consequently, a sensory evaluation would provide a global acceptability score, but the product may also be analyzed for quality using objective measurements of color or texture.

The principle by which apple puree turns into a flexible material by drying is the high methoxyl pectin–sugar–acid gelation. Gelation takes place at pH 3–3.5 once the soluble solids content (notably sugars) reach 55 to 65% *w/w*. This mechanism was described by Rolin and De Vries (1990) during cooking of jam and can be extrapolated to dehydration. At the beginning of drying, sugar and pectins are well hydrated but, as drying proceeds, sugar concentrates and “competes” with pectin for water. At low-moisture contents, a network is formed by junctions between pectin molecules entrapping a concentrated sugar solution. These gels are not thermoreversible.

There is scarce information on the formulations and drying-related properties, which would assist process design. Therefore, the general objective of this study was to characterize the formation process of apple pectic gels by hot-air drying. The specific objectives were (1) to characterize the product by determining and modeling drying-related physical and physico-chemical properties such as the desorption isotherm, volume, and density as a function

of moisture content; (2) to experimentally determine and model drying kinetics, as far as possible, with a model having physical meaning yet of manageable complexity.

Materials and Methods

Preparation of Samples for Drying

Apples *var.* Granny Smith were purchased in a local market and stored at 10 °C for 24 h before use. Fruits were washed with drinking water, peeled, cut in halves, cored, cut into 14-mm dices, and steam-blanching (400 g of sample over 4,800 ml of boiling water at atmospheric pressure) for 600 s to avoid enzymatic browning, to soften the tissues and to allow pectins to be dissolved and distributed before gelation.

As the use of blanched apple puree alone led to a poor-quality dehydrated pectic gel, 79 g of puree was added with 18 g of sucrose and 3 g of an aqueous solution of citric acid (0.174% *w/w*) per 100 g of formulation before drying to enhance the pectin–sugar–acid gelation (Moreno Semhan et al. 2004). Moreover, the use of citric acid provided an extra hurdle to microbial growth (Andrés et al. 2002). The blanched apple dices (average moisture content, 85.7% *w.b.* or 5.992 *dec., d.b.*) were pureed and mixed with the ingredients in an electric blender (Braun Multiquick Advantage, MR-4050, Spain) for 2 min. The initial formulation for drying had a moisture content of 70.6% *w.b.* or 2.402 *dec., d.b.*

Determination of Moisture Content and pH

Moisture content was determined in a vacuum oven by the Association of Official Analytical Chemists (AOAC) technique 22.018 (AOAC 1984). Replicates did not differ by more than 0.003 *dec., d.b.* The pH was determined by the AOAC 22058 method (AOAC 1984). All measurements were carried out in triplicate.

Rapid Water Activity Measurements

Rapid water activity determinations of the initial formulation and finished product were carried out at 25 °C by the hygrometric method in an Aqualab 3TE meter (Decagon Devices, Inc., USA). Moisture content of samples was verified later by the vacuum oven method, as described in “Determination of Moisture Content and pH.” All measurements were carried out in triplicate.

Determination of the Desorption Isotherm

The desorption isotherm was determined at 25 °C according to the static gravimetric method described by Labuza

(1984) by equilibrating the initial formulation with 11 saturated solutions. These solutions with their specific water activities given in parenthesis were NaOH (0.069), LiCl (0.111), KCH₃COO (0.237), MgCl₂ (0.328), K₂CO₃ (0.432), MgNO₃ (0.536), NaNO₂ (0.645), NaCl (0.753), KCl (0.843), BaCl₂ (0.904), and K₂SO₄ (0.973). Triplicate determinations were carried out for each saturated solution.

The equilibrium attained after three consecutive weighings in analytical balance did not differ by more than 0.001 g, taking from 3 to 4 weeks. The resulting moisture content of each sample was determined as indicated in “Determination of Moisture Content and pH.”

Volumetric Shrinkage and Density

Food tissues and gel foods experience considerable shrinkage during hot-air drying (Ratti 1994; Bhandari and Howes 1999). This is because the process evolves while the material is in its rubbery region (Roos 1995). As water is removed in hot-air drying, the material cannot withstand its own weight and collapses; this aspect often reduces organoleptic quality in cellular foods, although not in pectic gels.

During drying, the apple formulation changes from a fluid-like appearance to a soft paste texture and, finally, to a firm gel. To study the volume variation, the initial formulation was placed into acrylic trays (0.18 m long by 0.138 m wide by 0.013 m high), with an initial thickness of 6×10⁻³ m, and was dehydrated at 60 °C in a forced convection oven to several moisture contents. Ochoa et al. (2002) have found that volume and area changes are independent from drying conditions and only related with the product moisture content.

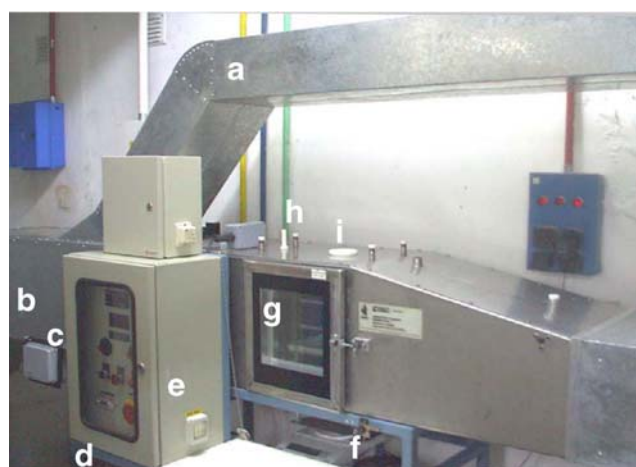


Fig. 1 Stainless steel tray dryer for kinetic drying experiments. **a** Parallel duct, **b** internal resistance elements, **c** by-pass valve, **d** automatic air temperature controller, **e** air velocity controller, **f** precision digital balance, **g** drying chamber, **h** temperature sensors, **i** orifice for taking non-contact product temperature measurements

For each moisture, the sample thickness was measured with the depth probe of a Vernier caliper (readability, 0.1 mm) at six positions in the tray; the results were averaged. The product surface area was measured with a precision ruler (readability, 0.5 mm). Density was calculated from the product volume and the product mass, the latter being determined in an OHAUS Adventurer digital balance (maximum weighing capacity, 1,500 g; readability, 0.01 g; OHAUS Corp., USA). Determinations were conducted in triplicate.

Kinetic Drying Experiments

Experimental Drying Technique

Room dry and wet bulb temperatures were measured with a purpose-built, Assmann-type aspirated psychrometer (air velocity, 4 m/s) and supplied to a psychrometric chart software (Akton Associates Inc., USA) to find the air absolute humidity (h_a). With this value and the drying air temperature, T_a , the drying air relative humidity, h_r , was also calculated via software. The moisture content in the initial formulation was determined by the vacuum oven technique, as explained in “Determination of Moisture Content and pH.”

The drying kinetic experiments were carried out in a purpose-developed stainless steel tray dryer (Fig. 1) with insulated walls. The drying chamber contained a framework holding up to three trays 0.20×0.20 m side. The initial product thickness in the tray was 6×10^{-3} m. The tray with the sample was placed in the dryer, and the measurement of a drying curve began. Weighings were carried out in situ at several times, t , during drying using another OHAUS precision digital balance (readability, 0.01 g; capacity, 3,100 g). To avoid weighing instabilities caused by the airflow, a by-pass valve diverted the air current to a parallel duct running above the dryer while the framework was disengaged and deposited onto the balance. Once the mass m was read, the flow was restored again, and the framework lifted and engaged by a mechanism. The weighing procedure took about 15 s.

Except the initial value measured by the vacuum oven technique (see “Determination of Moisture Content and pH”),

the experimental moisture contents were determined from the weighings using a mass balance, assuming constant product dry matter (m_d) during drying.

$$W = \left(\frac{1 + W_0}{m_0} \right) m - 1 \quad (1)$$

where W and m are the moisture content (dec., d.b.) and product mass (kg), respectively, at a generic time t , whereas W_0 and m_0 are the corresponding initial values.

The product temperature curve was recorded with a non-contact, infrared thermometer Testo 830 T2 (readability, 0.1 °C; accuracy, ± 0.5 °C; Testo AG, Germany) by measuring from above, through an orifice in the dryer wall. The orifice was normally closed by a solid polypropylene plug. At the measuring times, the plug was removed to take several readings in a few seconds. Drying experiments were carried out in duplicate at air temperatures of 50, 60, and 80 °C, with a controlled air velocity of 2.0 ± 0.05 m/s. Air temperatures were automatically controlled by an electronic, proportional device to ± 0.5 °C of the target value, in turn measured with a Pt-100 thermoresistance. Power was supplied uniformly to all resistance elements at the same time (total power, 14.4 kW) to provide homogeneous air heating in the dryer cross-section.

The practical equilibrium moisture content at the drying conditions, W_e , was measured by prolonging the drying runs up to stable product weight (24 to 36 h after the beginning of drying). This asymptotic moisture content was considered by Bruce (1985) as more appropriate for drying modeling than the usually lower value provided by the desorption isotherms at the low relative humidities of the drying air.

Determination of the Effective Heat Transfer Coefficient in the Dryer

The tray-air heat transfer coefficient, h , was experimentally determined by an unsteady-state technique, solving for this purpose a macroscopic energy balance around the product. This method is useful because it provides an effective coefficient valid in actual experimental conditions. The

Table 1 Coefficients of the two equations fitted to experimental values of moisture content, W , (dec., d.b.) vs time, t (min); $W = a t^3 + b t^2 + c t + d$ and product temperature, T (°C), vs time, t (min): $T = a + b (1 - \exp(-c t^d))$

	T_a (°C)	a	b	c	d	r^2
Moisture content, W (dec., d.b.)	50	-0.849×10^{-8}	1.428×10^{-5}	-0.905×10^{-2}	2.377	0.999
	60	-1.122×10^{-8}	1.957×10^{-5}	-1.156×10^{-2}	2.450	0.999
	80	-2.797×10^{-8}	3.484×10^{-5}	-1.504×10^{-2}	2.393	0.999
Product temperature, T (°C)	50	16.886	-5.443	-0.934	0.119	0.993
	60	16.792	-5.564	-1.087	0.114	0.996
	80	17.069	-0.606	-3.312	0.0578	0.999



Fig. 2 Appearance of the finished product: apple pectic gel. Moisture content=0.269, pH=3.4, water activity=0.692, and thickness= 2×10^{-3} m

technique was proposed for foods by Ratti and Crapiste (1995). The equation used was as follows:

$$h = \frac{m_d(1+W)C_p \frac{dT}{dt} + L_{wd}m_d \left(-\frac{dW}{dt}\right)}{(T_a - T)A} \quad (2)$$

where T_a is the air temperature in the dryer chamber and T the average product temperature at time t . In turn, L_{wd} is the heat of desorption of water and A the transfer area. The symbols $\frac{dT}{dt}$ and $\frac{dW}{dt}$ are the first derivatives of the four-parameter empirical correlations for moisture content and temperature as a function of time (see Table 1). These correlations were fitted with the sole purpose of calculating their derivatives.

As no correlation for the specific heat of apple laminates was found, an expression for whole apples provided by Mohsenin (1980) was employed.

$$C_p = 836.8 + 3347.2 \left(\frac{W}{1+W}\right) \quad (3)$$

Sensory Evaluations

The pectic gel produced after 400 min of tray drying at 60 °C was evaluated by 40 untrained panelists in parameters as appearance, color, taste, texture, and general acceptability. A hedonic descriptive scale of five points was utilized.

Results and Discussion

The initial formulation had a water activity $a_w=0.966$ and a pH=3.34. The aim was to find a firm, dehydrated gel product microbially safe at room temperature ($a_w<0.7$). A photograph of the finished product (moisture content=0.269 dec., d.b.; water activity, 0.692 (measured as indicated

in “Determination of the Desorption Isotherm”; pH=3.40) is displayed in Fig. 2. The pectic gel has a moisture content below the maximum of 0.333 dec., d.b. allowed in Argentina for dehydrated fruit and fruit products (CAA 2004).

Volumetric Shrinkage

Shrinkage of pectic gels during drying was one-dimensional because the relative reduction in thickness was considerably more important than in surface area. Moreover, the product retained its plane sheet shape unaltered during drying. This behavior agreed with that observed for other gels by Kechaou et al. (1987).

The following theoretical model was deduced:

$$V = V_0 - a V_{wev} \quad (4)$$

where V_0 is the initial volume, and a is a parameter varying between 0 and 1. Mayor and Sereno (2004) have stated that materials undergoing water removal tend to reach mechanical equilibrium when shrinkage equals the volume of removed water. By assuming this behavior, $a=1$. The volume of water evaporated is $V_{wev}=m_{wev}/\rho_w$, whereas m_{wev} stands for the mass of water evaporated and ρ_w for the density of liquid water. Assuming constant dry matter, m_d , the mass of water evaporated can be calculated by the following expression:

$$m_{wev} = m_d(W_0 - W) \quad (5)$$

where $W_0=2.23$ dec., d.b.

Therefore, the expression of volume as a function of moisture content becomes

$$V = V_0 - \left(\frac{m_d(W_0 - W)}{\rho_w}\right) \quad (6)$$

Replacing m_d by $\rho_d V_d$, and V_0 by $V_d+(\rho_d V_d W_0/\rho_w)$ (the volume of the dry solid plus the initial water volume in the product), dividing both members by V_0 and rearranging the final expression for V/V_0 as a function of W is obtained.

$$\frac{V}{V_0} = \left[1 - \frac{W_0}{\rho_w \left(\frac{1}{\rho_d} + \frac{W_0}{\rho_w}\right)}\right] + \left[\frac{1}{\rho_w \left(\frac{1}{\rho_d} + \frac{W_0}{\rho_w}\right)}\right] W \quad (7)$$

The value of ρ_d , the dry matter density, was determined by pycnometry to be 1,382 kg/m³. The theoretical intercept was 0.245, representing the fraction of the initial volume that would remain in the totally dehydrated product. The results of this model (Eq. 7) were plotted together with the experimental values in Fig. 3. Agreement was excellent, so the mechanism proposed in this study provides a correct description of shrinkage.

This linear dependence of volume reduction with moisture content was used to calculate product density and laminate thickness for the study of drying kinetics.

Density

The product density $\rho = m/V = m_d(1 + W)/V$ was calculated by an expression based on Eq. 7. The product volume at any moisture content W is $V = V_d + V_w$, i.e.,

$$V = \frac{m_d}{\rho_d} + \frac{m_d W}{\rho_w} = m_d \left(\frac{1}{\rho_d} + \frac{W}{\rho_w} \right) \tag{8}$$

Thus, replacing Eq. 8 in the density formula, a preliminary expression is obtained:

$$\rho = \frac{m}{V} = \frac{m_d(1 + W)}{m_d \left(\frac{1}{\rho_d} + \frac{W}{\rho_w} \right)} \tag{9}$$

Finally, as m_d drops out from the equation and after multiplying the numerator and the denominator by ρ_d , the final expression for the product density is attained:

$$\rho = \frac{\rho_d(1 + W)}{1 + \frac{\rho_d}{\rho_w} W} \tag{10}$$

This density model was compared with averages of experimental data, and a satisfactory agreement can be observed in Fig. 4. Density increases as moisture decreases, particularly, at lower moisture contents. The density of the material changes from 1,084 kg/m³ in the initial formulation to $\rho_d=1,382$ kg/m³ for the totally dehydrated product

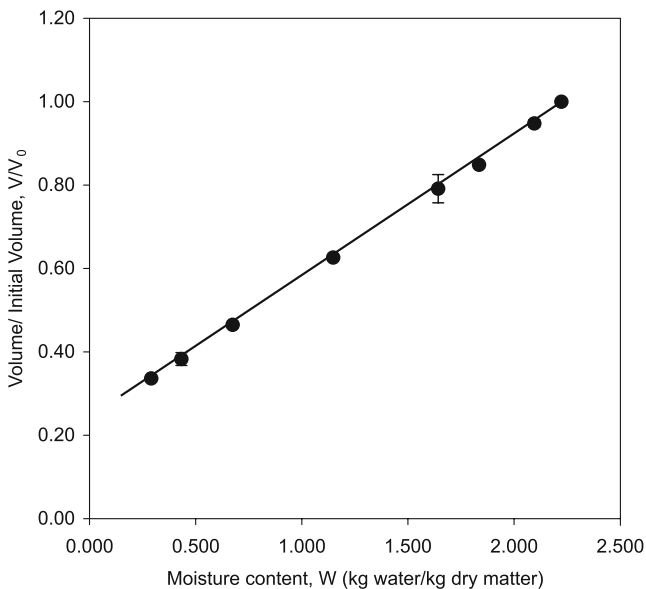


Fig. 3 Normalized volume as a function of moisture content. Circle Experimental data and line predictions by the theoretical shrinkage model

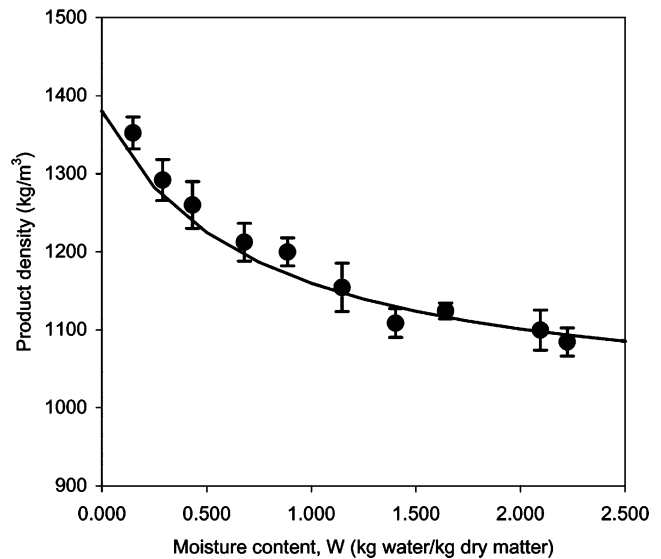


Fig. 4 Product density as a function of moisture content. Circle Experimental densities and line model-predicted values

(maximum shrinkage). As the dry solid is denser than liquid water, this behavior is observed in the presence of collapse: The higher the solids concentration, the higher the density. The average relative error of predictions was 1.36%.

Desorption Isotherm

The isotherm may be utilized to determine, at a given value for a_w , e.g., 0.7, the final moisture content of drying, which is a determinant factor of the drying time. Figure 5 exhibits the average experimental data, and their standard deviation of the desorption isotherm measured at 25 °C. The curve was J-shaped, type III in the BET classification (Gregg and Sing 1967) typical of sugar-rich products. At water activities higher than 0.65, moisture content sharply increases with water activity because more sugar dissolves and increases water retention.

The sorption isotherm model of Halsey (Eq. 11), GAB (Eq. 12), and Oswin (Eq. 13), tested by Kaya and Kahyaoglu (2005) in a study of thermodynamic properties and sorption equilibrium of pestil (grape leather), were also utilized in this study to describe the experimental data.

$$a_w = \exp\left(\frac{-A_h}{WB_h}\right) \tag{11}$$

$$W = \frac{W_m C k a_w}{(1 - k a_w)(1 - k a_w + C k a_w)} \tag{12}$$

$$W = A_o \left(\frac{a_w}{(1 - a_w)} \right)^{B_o} \tag{13}$$

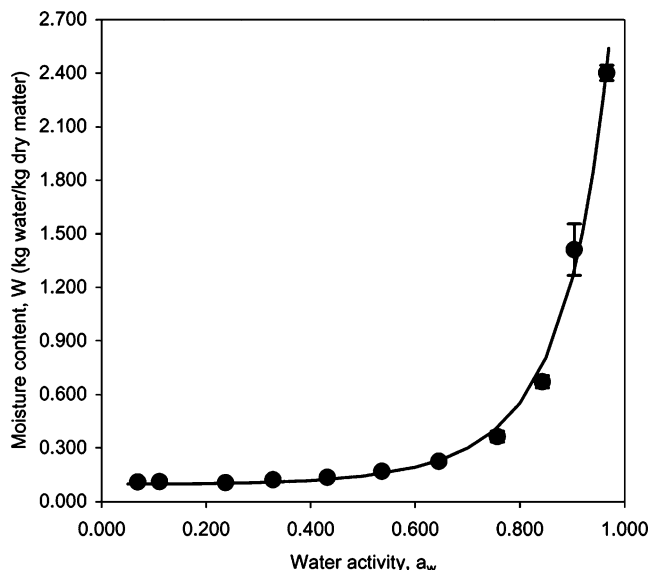


Fig. 5 Product sorption isotherm at 25 °C. Circle Experimental values and line calculated data by a newly proposed model $W = 0.0994 \exp(3.584 a_w^{3.307})$

Besides, a new sorption equation suitable for steep exponential-shaped curves was tested

$$W = C_1 \exp(C_2 a_w^{C_3}) \tag{14}$$

The fitting parameters of the models were determined by nonlinear least squares in a statistical software (Systat 1990) and are listed in Table 2. Standard deviations of the parameters are given in parenthesis. Equation (14) was selected based on the coefficient of determination (r^2). This isotherm expression was also the most practical because of its higher accuracy in the a_w range of 0.65–0.85, which is critically important for food safety. The safe moisture content was calculated by Eq. 14 for a water activity of 0.7 to be

Table 2 Fitting parameters and goodness of fit indices of Halsey, Oswin, GAB, and a new model for the desorption isotherm at 25 °C

	Halsey	GAB	Oswin	New sorption equation
A_h	0.11029 (9.08 × 10 ⁻³) ^a			
B_h	1.276 (0.0952)			
r^2	0.969	0.978	0.973	0.995
K^b		0.976		
C		3.949		
W_m		0.142		
A_o			0.217 (0.0359)	
B_o			0.726 (0.0545)	
C_1				0.0994 (0.0239)
C_2				3.584(0.229)
C_3				3.307 (0.376)

^a Asymptotic standard error of each parameter

^b The software did not report standard deviation of parameters in this case.

Table 3 Operating conditions for the drying experiments

Drying air temperature, T_a (°C)	Absolute humidity, h_a (kg vapor/kg dry air)	Relative humidity of the drying air, h_r , dec.	Equilibrium moisture content, W_e (dec., d.b.)
50	0.0103	0.135	0.0934
60	0.0106	0.086	0.0752
80	0.0093	0.0318	0.0284

0.299 dec., d.b. (23.02% w.b.). This equation is an empirical mathematical correlation with the ability of dealing with sharply changing slopes using only three parameters. In sorptional equilibrium, it is suitable for solute-rich materials.

Drying Kinetics

Experimental Data

Table 3 lists, for each drying condition, the drying air temperature, absolute humidity, relative humidity, and the equilibrium moisture content. Figure 6 shows the experimental dimensionless product moisture content $W_{ad} = (W - W_e)/(W_0 - W_e)$, as a function of time t (minutes) at the three drying air temperatures covered. Moisture content rapidly decreases at the beginning of drying and then varies more slowly, as expected for a material approaching equilibrium conditions.

Figure 7a, in turn, shows the drying mechanism curve, where the drying rate was plotted as a function of moisture content (Barbosa-Cánovas and Vega-Mercado 1996). Drying

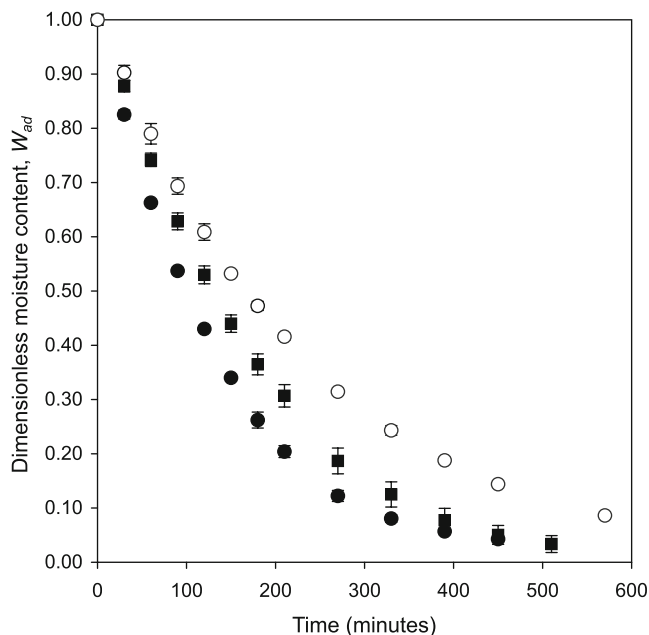


Fig. 6 Experimental values of the dimensionless moisture content (W_{ad}) as a function of time at 50 °C (open circle), 60 °C (square), and 80 °C (filled circle)

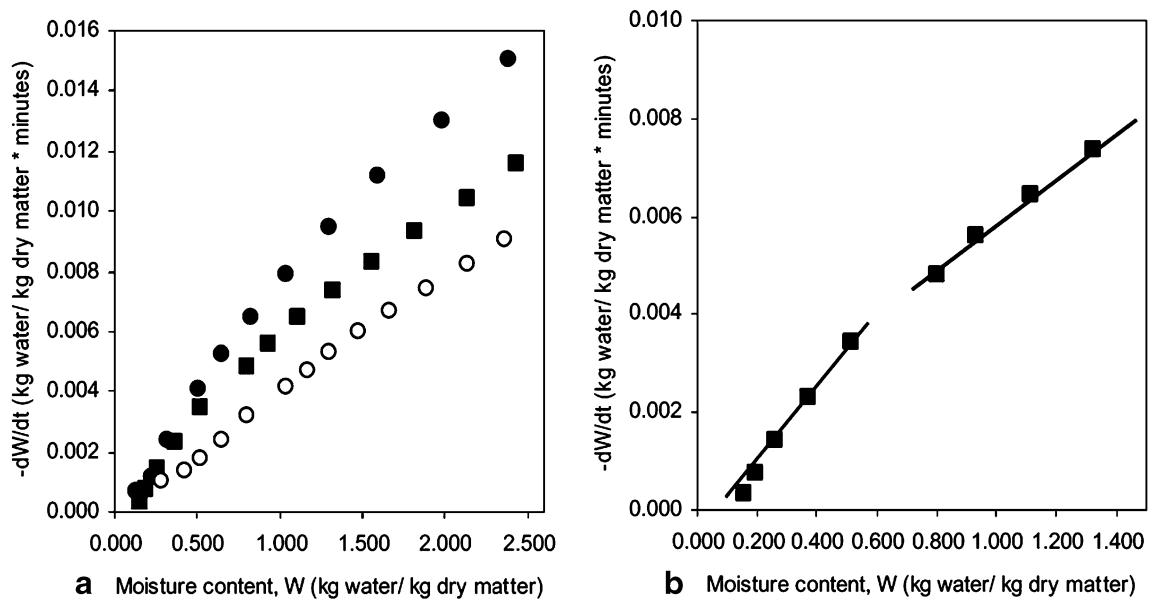


Fig. 7 a Overall graph of drying rate vs moisture content: 50 °C (open circle), 60 °C (square), and 80 °C (filled circle). b The low- and high-moisture regions in a magnified view of the drying rate graph at 60 °C

rates increase with air temperature but is observed to decrease continuously along each drying experiment. Therefore, the whole process occurs in the falling drying rate period. The drying process was divided in two zones for each temperature: high-moisture (hm) and low-moisture (lm) (Pezzutti and Crapiste 1997). To clarify the division method, Fig. 7b shows a magnified view of the same graph at 60 °C with the separation between the zones. This occurred for a moisture content of about 0.8 dec., d.b.

Drying Model for the High-Moisture Zone

Model Description Crapiste and Rotstein (1997) provided a contribution to drying design by describing analytical solutions of the diffusion equation that can be utilized to study the drying kinetics of foods in isothermal systems. In addition to mass transfer, many researchers suggested to consider heat transfer modeling when studying drying kinetics (Vagenas and Marinos-Kouris 1990).

A suitable model for internal–external control of the mass transfer rate is the analytical solution of the transient microscopic mass balance integrated over a plane sheet. This infinite series for isothermal drying (Crank 1975; Pezzutti and Crapiste 1997; Crapiste and Rotstein 1997) is written below:

$$W_{ad} = \frac{W - W_e}{W_0 - W_e} = \sum_{n=1}^{\infty} \frac{2Bi^2 \exp\left(\frac{-\beta_n^2 D_{hm} t}{d_{hm}^2}\right)}{(\beta_n^2 + Bi^2 + Bi)\beta_n^2} \quad (15)$$

where β_n is the n th root of the transcendental equation $\beta_n \tan \beta_n - Bi = 0$. The symbol Bi represents the mass transfer Biot number. The symbol d_{hm} is the average product thickness in the high-moisture zone calculated with the shrinkage model (Eq. 7), whereas D_{hm} is the effective diffusion coefficient in the high moisture zone.

Although the model assumes no change of D_{hm} with concentration and constant product volume, the use of an average d_{hm} should considerably reduce prediction errors,

Table 4 Parameters for the correlation $\beta_n = M_{1n}(1 - \exp(-M_{2n} Bi^{M_{3n}})) + M_{4n}$ of the first six roots of the transcendental equation $\beta_n \tan \beta_n - Bi = 0$, with the Biot number, Bi

	Parameters of the correlation between β_n and Bi				r^2
	M_{1n}	M_{2n}	M_{3n}	M_{4n}	
β_1	1.494	0.855	0.564	0	1.000
β_2	1.532	0.222	0.838	3.129	0.999
β_3	1.497	0.117	0.941	6.279	1.000
β_4	1.464	0.077	0.995	9.424	1.000
β_5	1.434	0.057	1.023	12.566	1.000
β_6	1.407	0.046	1.038	15.708	1.000

as it leads to the fitting of an average value for D_{hm} in the high-moisture zone.

This meaningful model (Eq. 15; Crank 1975) was seldom employed in the literature, possibly because of lack of information on its use. Pezzutti and Crapiste (1997), for garlic drying, were among the few who utilized this diffusive model. However, they considered isothermal drying and used only one term of Eq. 15, which is correct only at long times.

As drying of high-moisture foods as pectic gels is non-isothermal (Mulet 1994), a coupled heat and mass transfer model is required. Thus, a nonlinear ordinary differential equation (ODE) system in an initial value problem was proposed, which consists of Eq. 16 (the derivative of Eq. 15 with respect to time) and the macroscopic energy balance in the product (Eq. 17). Temperature gradients inside the product are neglected, as heat conduction is hundreds to thousands of times faster than moisture diffusion (Mohsenin 1980). Therefore, the drying model takes the following form:

$$\frac{dW}{dt} = -2 \text{Bi}^2 (W_0 - W_e) \left[\sum_{n=1}^{\infty} \frac{1}{(\beta_n^2 + \text{Bi}^2 + \text{Bi}) \beta_n^2} \left(\frac{\beta_n^2 D_{hm}}{d_{hm}^2} \right) \exp \left(\frac{-\beta_n^2 D_{hm} t}{d_{hm}^2} \right) \right] \quad (16)$$

$$\frac{dT}{dt} = \frac{h A (T_a - T) - L_{wd} \left(-\frac{dW}{dt} \right) m_d}{m_d (1 + W) C_p} \quad (17)$$

where the initial conditions are $t=0$, $W=W_0$, and $T=T_0$.

The average thickness d_{hm} in the high-moisture zone was calculated to be 4.67×10^{-3} m using Eq. 7 at the mean moisture content of the high-moisture zone, 1.707 dec., d.b.

The non-isothermal analysis is carried out in the high-moisture zone, where the heat of desorption, L_{wd} , and the latent heat of vaporization of pure water, L_w , are almost equivalent. Moreover, in high-sugar products, the net effect of temperature on the desorption isotherm is very small and determines an almost null difference between L_{wd} and L_w (Kayman-Ertekin and Gedik 2004). The value of L_w was used, which was calculated by a temperature-dependent thermodynamic expression described by Giner and Gely (2005).

Equation 2 was solved to determine the heat transfer coefficients for each air-drying temperature. By averaging them, a mean heat transfer coefficient was obtained to be 40.9 ± 2.24 W/m² °C, which was in close agreement with the values reported by Ratti and Crapiste (1995) for potato-slice drying in parallel plates. This value was used in Eq. 17.

The coupled ODE system (Eqs. 16 and 17) must be numerically solved in an inverse problem to determine the effective diffusion coefficients and a representative mass transfer Biot number.

Algorithm for Determining the Diffusion Coefficient in the High-Moisture Zone The fitting of the diffusion coefficient in the high moisture zone is complicated in each drying experiment because the transport parameter must be determined from a system of two ordinary differential equations. Therefore, the procedure was divided in two steps. In the first, the integral form of the analytical solution for isothermal drying (Eq. 15) was fitted to the data of moisture content vs time to find the optimum mass transfer Bi, the corresponding diffusion coefficients D_{hm} , and the preliminary relationship between D_{hm} and air temperature.

To utilize Eq. 15, the first six roots of the transcendental equation $\beta_n \text{tg } \beta_n - \text{Bi} = 0$ provided by Crank (1975) were related here with the mass transfer Biot numbers between 0 and ∞ by the proposed correlation:

$$\beta_n = M_{1n} (1 - \exp(-M_{2n} \text{Bi}^{M_{3n}})) + M_{4n} \quad (18)$$

where $n=1 \dots 6$

Table 4 lists the fitting parameters M_{1n} , M_{2n} , M_{3n} , and M_{4n} , and the index of goodness of fit. Agreement was excellent for all Biot numbers.

A Matlab program was developed where Eq. 18 was included in Eq. 15 for determining the diffusion coefficient for values of Bi between 0.5 and 4. At each Biot, a diffusion coefficient was found, which minimized the sum of squares of the deviations (MSS) between predicted and experimental moisture contents. Once all Biots in each drying curve and all the drying curves (i.e., all drying temperatures) were processed, a procedure to select a single value of the mass transfer Biot was devised. To this end, the sums of MSS for the various drying temperatures were calculated at each Biot number; representative Biot number was that for which the sum of MSS was minimum. The mass transfer Biot number for the drying of apple pectic gels was 2.1. The procedure was plotted in Fig. 8. The optimum mass transfer Biot number indicates that, on average, the internal resistance to mass transfer was about twice as high as the external resistance in the high-moisture zone. Few previous works attempted to calculate mass transfer Biot numbers for food drying processes (Pezzutti and Crapiste 1997). The diffusion coefficients corresponding to $\text{Bi}=2.1$ were correlated with air temperature by a preliminary Arrhenius expression,

$$D_{hm} = D_{0hm} \exp \left[\frac{-E_{ahm}}{R (T + 273.16)} \right] \quad (19)$$

to find $D_{0hm} = 3.673 \times 10^{-7}$ m²/s, $E_{ahm} = 15,259$ J/mol, and $r^2 = 0.974$.

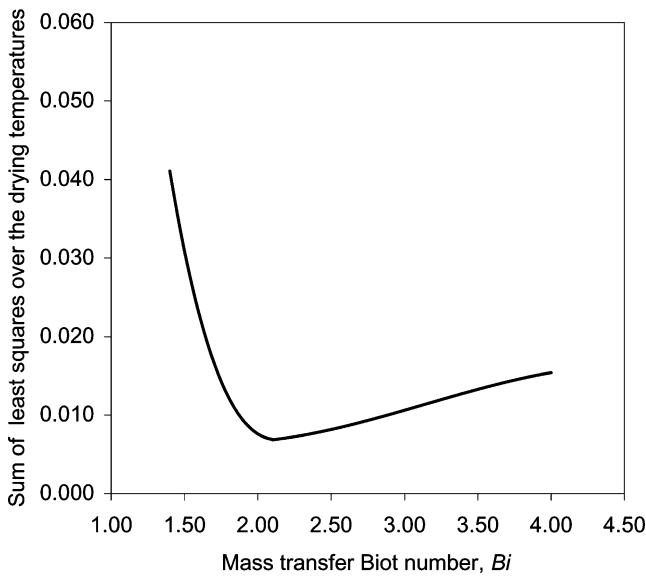


Fig. 8 Sum of least squares of deviations between predicted and experimental moisture contents at the four temperatures for the kinetic model in the high-moisture zone, plotted as a function of the mass transfer Biot number

The second step of the fitting was carried out by solving the EDO system (Eqs. 16 and 17) by the fourth order Runge–Kutta method (Constantinides and Mostoufi 1999). The optimum value, $Bi=2.1$, and the activation energy of 15,259 J/mol were retained for these calculations. The optimization criterion was, again, to minimize the sum of squares of deviations between predicted and experimental moisture contents, modifying the preexponential factor by a multiplier (f) to convert an Arrhenius equation based on the air temperature to an expression based on the variable product temperature. Table 5 lists the information on the fitting procedure. The optimizing value of f was 1.4, so the final preexponential factor was $D'_{0hm}=5.142 \times 10^{-7} \text{ m}^2/\text{s}$. This higher parameter compensated for the lower product temperatures utilized in the non-isothermal model (Eqs. 16

and 17) compared with the air temperatures employed in the isothermal expression (Eq. 15). The activation energy was in close agreement with the values published by Maskan et al. (2002) for pestil (grape leather).

Figure 9a–c shows the average values of experimental product moisture content and temperature vs time, and their corresponding prediction lines at 50, 60, and 80 °C. Calculations are observed to represent satisfactorily the experimental behavior. The average computed r^2 was 0.988 for the moisture content curves. The figures show that product temperature is definitely lower than air temperature in the high-moisture zone, and this feature is utilized by food processors to employ higher air temperatures at the beginning of drying, reducing it toward the end to avoid quality deterioration (Greensmith 1998).

Low-Moisture Zone

The mass transfer control in the low-moisture zone is totally internal, and isothermal drying can be assumed to occur at the air temperature (Crapiste and Rotstein 1997). The moisture content at the surface is considered equal to the equilibrium moisture content (see Table 2), and the analytical solution becomes independent from the Biot number. As the low-moisture zone occurs at long drying times, a one-term expression of the infinite series for plane sheets can be utilized (Crapiste and Rotstein 1997; Nguyen and Price 2007):

$$W_{ad} = \frac{W - W_e}{W_0 - W_e} = \frac{8}{\pi^2} \exp\left(-\frac{\pi^2}{4} \frac{D_{lm} t}{d_{lm}^2}\right) \tag{20}$$

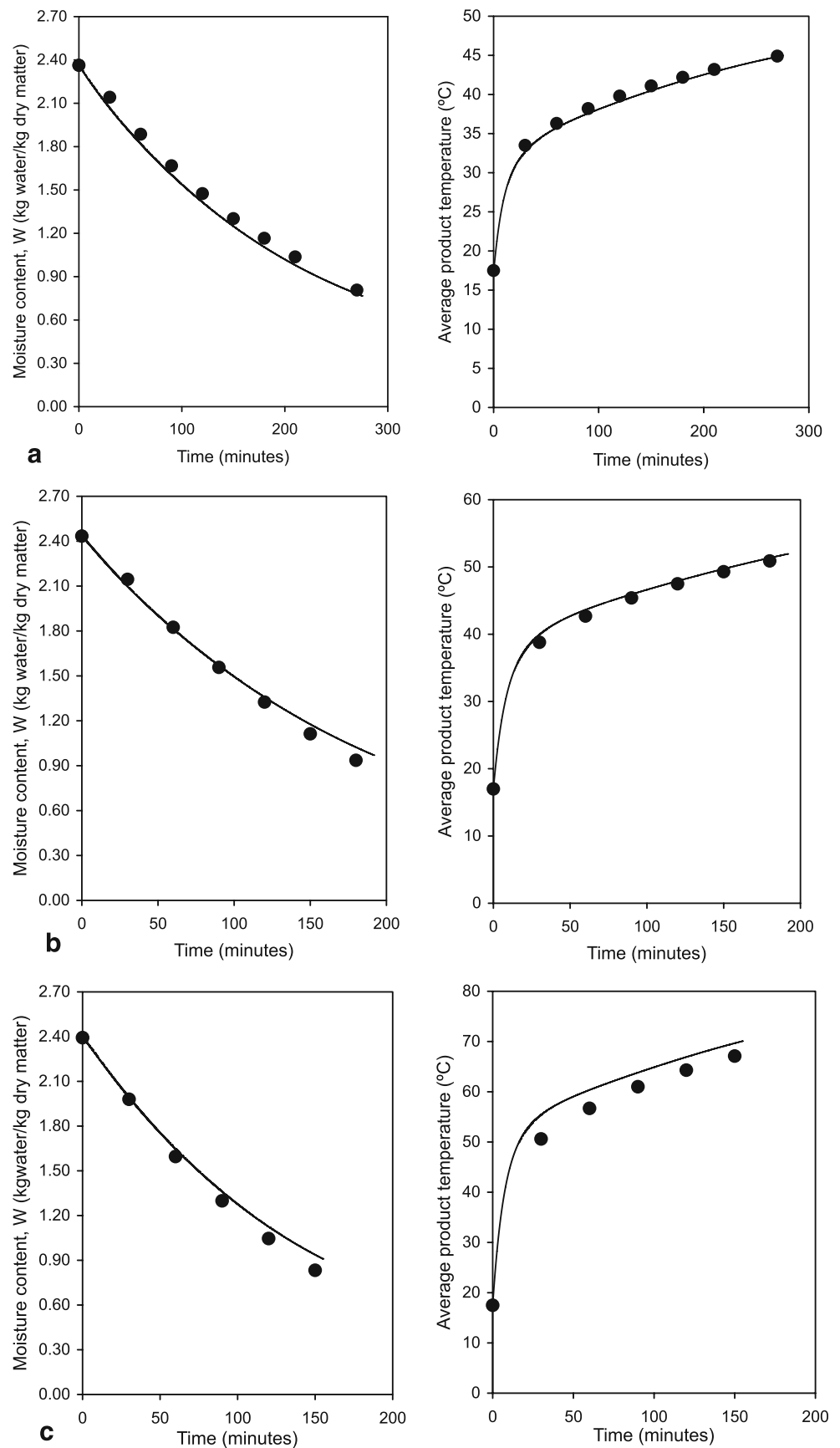
The average product thickness d_{lm} in the low-moisture zone was calculated by Eq. 9 to be $2.24 \times 10^{-3} \text{ m}$.

The diffusion coefficients D_{lm} were obtained by least-squares fitting of Eq. 20 to the curve of moisture content vs

Table 5 Multiplier (f) of the preliminary Arrhenius preexponential factor and sum of squares of the deviations (MSS) in the coupled heat and mass transfer drying model for $Bi=2.1$ in the high-moisture zone

f	Drying air temperature T_a (°C)						Total sum of MSS at four temperatures
	50		60		80		
	$D \times 10^9 \text{ (m}^2/\text{s)}$	MSS	$D \times 10^9 \text{ (m}^2/\text{s)}$	MSS	$D \times 10^9 \text{ (m}^2/\text{s)}$	MSS	
0.70	0.801	0.6942	0.921	0.8175	1.239	0.8077	2.3194
1.00	1.139	0.1232	1.294	0.2572	1.746	0.2768	0.6572
1.20	1.369	0.0121	1.546	0.0850	2.093	0.1051	0.2022
1.30	1.487	0.0079	1.674	0.0397	2.269	0.0551	0.1027
1.40	1.605	0.0290	1.803	0.0154	2.449	0.0233	0.0677
1.50	1.755	0.0702	1.934	0.0086	2.631	0.0064	0.0852
1.60	1.847	0.1272	2.067	0.0162	2.816	0.0017	0.1451
1.80	2.093	0.2755	2.337	0.0649	3.196	0.0180	0.3584
2.00	2.344	0.4526	2.615	0.1456	3.589	0.0637	0.6619

Fig. 9 Experimental moisture content and product temperature (filled circle) vs time for the high-moisture zone and the corresponding predicted lines for all the air temperatures studied: 50 °C (a), 60 °C (b), and 80 °C (c)



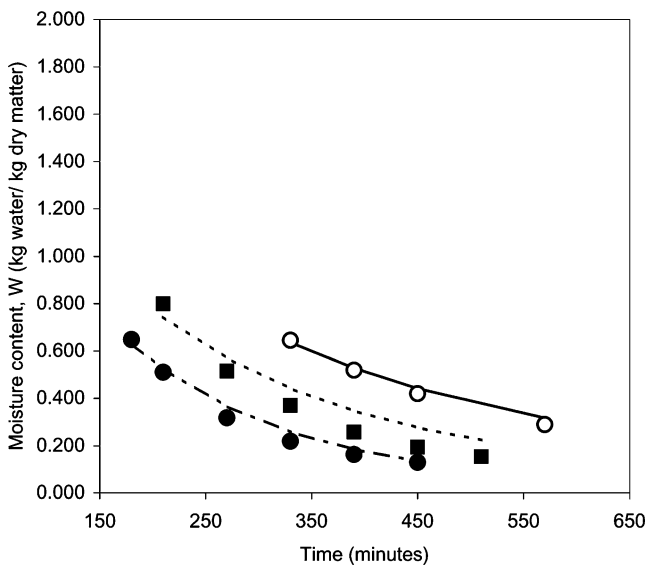


Fig. 10 Experimental product moisture content (*symbols*) vs time for the low-moisture zone and the corresponding predictions (*lines*) for all the air temperatures studied: 50 °C (○), (—); 60 °C (■), (- - -); and 80 °C (●), (- · - ·)

time using only the data belonging to this zone at the three temperatures. The average value of r^2 was 0.967. Agreement of predicted and observed data was good, as shown in Fig. 10. The diffusion coefficient increased strongly with temperature and followed the Arrhenius law,

$$D_{lm} = D_{0lm} \exp \left[\frac{-E_{alm}}{R(T + 273.16)} \right] \quad (21)$$

where $D_{0lm} = 6.970 \times 10^{-8} \text{ m}^2/\text{s}$, $E_{alm} = 16,800 \text{ J/mol}$, with $r^2 = 0.952$. Again, the activation energy was similar to that determined in previous works for the dry zone (Pezzutti and Crapiste 1997).

The diffusion coefficient at 60 °C was $18.04 \times 10^{-10} \text{ m}^2/\text{s}$ in the high-moisture region and $1.692 \times 10^{-10} \text{ m}^2/\text{s}$ in the low-moisture zone; i.e., they differed by an order of magnitude, in agreement with previous literature (Pezzutti and Crapiste 1997). At high moisture contents, the product is only partially collapsed, so diffusion is facilitated. As collapse and shrinkage are related phenomena, there must be a relationship between the average diffusion coefficient in each zone and its average thickness or, rather, with its average moisture content (Gekas and Lamberg 1991). In general, the diffusion coefficient tends to increase for higher temperatures and higher moisture contents (Krokida et al. 2004). The diffusion coefficients obtained in this study for the apple pectic gels (Fig. 11) are within the limits presented by Geankoplis (1993) for biological gels, and, as expected, somewhat higher than the values reported for food tissues by Zogzas et al. (1996).

Sensory Evaluation of the Product

The results from the sensory evaluation (hedonic scale of five points) were the following: overall appearance, 4.06 (0.76); taste, 3.97 (0.74); color, 4.13 (0.83); and texture, 4.00 (0.92), the standard deviation of each parameter being presented in parenthesis. Consequently, dehydrated apple pectic gels presented high acceptability and constitute a promising product.

Conclusions

A pectic gel (laminate) was formed by dehydrating a formulation of apple puree added with sucrose and citric acid, by the mechanism of sugar–acid–high methoxyl pectin gelation. The product was shaped in sheet-like form to reduce the drying time.

Product volume decreased linearly for decreasing moisture contents, and this behavior was described with excellent agreement by a theoretical model, assuming that volume reduction equals the volume of the water evaporated. This model does not include fitting parameters, depending only on dry solids density, water density, and product initial moisture content.

Product density increases with the decrease of moisture content, and this non-linear behavior was accurately predicted with a theoretical expression based on the shrinkage model.

The sorption isotherm at 25 °C was J-shaped, typical of sugar-rich products, being more accurately predicted by a

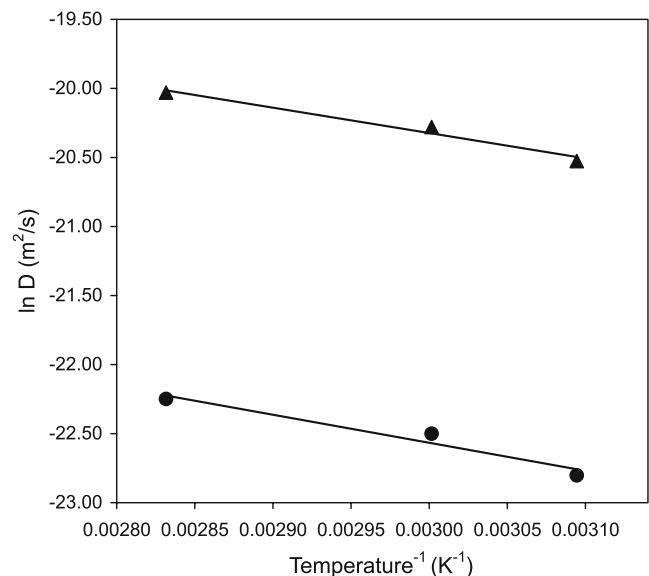


Fig. 11 Natural logarithm of the water diffusion coefficient in the apple pectic gels as a function of the reciprocal of the absolute temperature determined during the high- (*triangle*) and low- (*filled circle*) moisture zones. *Lines* indicate corresponding predictions by the Arrhenius equation

newly proposed phenomenological model for steep exponential curves than by the Halsey, GAB, and Oswin models.

The curves of moisture content vs time for apple pectic gels were predicted by two diffusional models, one for the high-moisture zone and another for the low-moisture region. In the former, a non-isothermal coupled mass and heat transfer model accurately predicts the experimental data. The mass transfer rate depended both on internal and external resistances, with a Biot number of 2.1. The temperature curve was predicted by integrating the macroscopic energy using an experimental heat transfer coefficient.

In the low-moisture zone, an isothermal diffusional mass transfer model with strict internal control was applied. The experimental diffusion coefficients fitted by the drying models followed an Arrhenius temperature dependence in both high- and low-moisture zones, with activation energies of 15,259 and 16,800 J/mol, respectively. Diffusion coefficients in the high-moisture zone (about 1×10^{-9} m²/s) were an order of magnitude greater than in the low-moisture region.

A sensory evaluation of the product (moisture content, 0.269 dec., d.b.; water activity, 0.692; and pH=3.4) showed high acceptability by a panel of consumers, scoring four out of five points in a hedonic scale.

Acknowledgment The authors thank Agencia Nacional de Promoción Científica y Tecnológica (ANPCyT), Argentina, for providing funding to Project PICT 2002 09-12196 and to the Comisión de Investigaciones Científicas, CICPBA, CONICET, and Universidad Nacional de La Plata from Argentina for their permanent support.

References

- Andrés, S. C., Giannuzzi, L., & Zaritzky, N. E. (2002). Quality parameters of packaged refrigerated apple cubes in orange juice. *Lebensmittel-Wissenschaft und-Technologie*, 35(8), 670–679.
- AOAC (1984). *Official methods of analysis* (14th ed.). Washington, DC, USA: Association of Official Analytical Chemists.
- Barbosa-Cánovas, G. V., & Vega-Mercado, H. (1996). *Dehydration of foods*. New York, USA: Chapman and Hall.
- Bhandari, B. R., & Howes, T. (1999). Implication of glass transition for the drying and stability of dried foods. *Journal of Food Engineering*, 40(1–2), 71–79.
- Bruce, D. M. (1985). Exposed-layer barley drying: three models fitted to new data up to 150°C. *Journal of Agriculture Engineering Research*, 32, 337–347.
- CAA (2004). *Código Alimentario Argentino, Cap. XI, Alimentos vegetales [Argentine Food Code, Ch. XI, Plant Foods]*. Administración Nacional de Medicamentos, Alimentos y Tecnología Médica. Ministerio de Salud y Ambiente de la Nación Argentina. Retrieved September 01, 2007 from <http://www.anmat.gov.ar/codigo/caa1.htm>.
- Constantinides, A., & Mostoufi, N. (1999). *Numerical methods for chemical engineers with MATLAB applications*. New Jersey, USA: Prentice Hall.
- Copley, M. J., & Van Arsdell, W. (1973). *Food dehydration, Vol. II. Products and technology*. Westport, CT, USA: The AVI Publishing.
- Crank, J. (1975). *The mathematics of diffusion* (2nd ed.). Oxford: Oxford University Press.
- Crapiste, G. H., & Rotstein, E. (1997). Design and performance evaluation of dryers. In K. J. Valentas, E. Rotstein, & R. P. Singh (Eds.) *Handbook of food engineering practice, Ch. 4* (pp. 125–165). Boca Raton, USA: CRC Press.
- Crapiste, G. H., Whitaker, S., & Rotstein, E. (1988a). Drying of cellular material—I. A mass transfer theory. *Chemical Engineering Science*, 43(11), 2919–2928.
- Crapiste, G. H., Whitaker, S., & Rotstein, E. (1988b). Drying of cellular material—II. Experimental and numerical results. *Chemical Engineering Science*, 43(11), 2929–2936.
- Geankoplis, C. J. (1993). *Transport processes and unit operations* (3rd ed.). New Jersey, USA: Prentice Hall.
- Gekas, V., & Lamberg, I. (1991). Determination of diffusion coefficients in volume-changing systems—Application in the case of potato drying. *Journal of Food Engineering*, 14(4), 317–326.
- Giner, S. A., & Gely, M. C. (2005). Sorptional parameters of sunflower seeds of use in drying and storage stability studies. *Biosystems Engineering*, 92(2), 217–227.
- Greensmith, M. (1998). *Practical dehydration* (2nd ed.). England: Woodhead.
- Gregg, S. J., & Sing, K. S. W. (1967). *Adsorption, surface area and porosity*. London: Academic.
- Kaya, S., & Kahyaoglu, T. (2005). Thermodynamic properties and sorption equilibrium of pestil (grape leather). *Journal of Food Engineering*, 71(2), 200–207.
- Kayman-Ertekin, F., & Gedik, A. (2004). Sorption isotherms and isosteric heat of sorption for grapes, apricots, apples and potatoes. *Lebensmittel-Wissenschaft und Technologie*, 37, 429–438.
- Kechaou, N., Roques, M. A., & Lambert, J. F. (1987). Diffusion in shrinking media: The case of drying of gels. In *Physical properties of foods-2, Part. 1: Diffusion, paper 4* (pp. 55–60). London: Elsevier Applied Science.
- Krokida, M. K., Foundoukidis, E., & Maroulis, Z. (2004). Drying constant: Literature data compilation for foodstuffs. *Journal of Food Engineering*, 61(3), 321–330.
- Krokida, M. K., & Marinos-Kouris, D. (2003). Rehydration kinetics of dehydrated products. *Journal of Food Engineering*, 57(1), 1–7.
- Labuza, T. P. (1984). *Practical aspects of isotherm measurement and use*. St. Paul, MN: American Association of Cereal Chemists.
- Maskan, A., Kaya, S., & Maskan, M. (2002). Hot air and sun drying of grape leather (pestil). *Journal of Food Engineering*, 54(1), 81–88.
- Mayor, L., & Sereno, A. M. (2004). Modelling shrinkage during convective drying of food materials: a review. *Journal of Food Engineering*, 61(3), 373–386.
- Mohsenin, N. M. (1980). *Thermal properties of food and agricultural materials*. London: Gordon and Breach.
- Moreno Semhan, D., Albertario, E., & Giner, S. A. (2004). *Dehydration of apple and tomato purees into flexible laminates. Heat and mass transfer studies and product characteristics. Drying 2004, Proceedings of the 14th International Drying Symposium (IDS 2004), Sao Paulo, Brazil, vol. C, pp. 1751–1758*.
- Mulet, A. (1994). Drying modelling and water diffusivity in carrots and potatoes. *Journal of Food Engineering*, 22(1–4), 329–348.
- Nguyen, M. H., & Price, W. E. (2007). Air-drying of banana: Influence of experimental parameters, slab thickness, banana maturity and harvesting season. *Journal of Food Engineering*, 79(1), 200–207.
- Ochoa, M. R., Kessler, A. G., Pirone, B. N., Márquez, C. A., & De Michelis, A. (2002). Shrinkage during convective air drying of whole rose hip (*Rosa rubiginosa* L.) fruits. *Lebensmittel-Wissenschaft und-Technologie*, 35(5), 400–406.
- Pezzutti, A., & Crapiste, G. H. (1997). Sorptional equilibrium and drying characteristics of garlic. *Journal of Food Engineering*, 31(1), 113–123.
- Ratti, C. (1994). Shrinkage during drying of foodstuffs. *Journal of Food Engineering*, 23(1), 91–105.

- Ratti, C. (2001). Hot air and freeze-drying of high value foods: A review. *Journal of Food Engineering*, 49(4), 311–319.
- Ratti, C., & Crapiste, G. H. (1995). Determination of heat transfer coefficients during drying of foodstuffs. *Journal of Food Process Engineering*, 18, 41–53.
- Rolin, C., & De Vries, J. (1990). Pectin. In P. Harris (Ed.) *Food gels* (pp. 401–434). Amsterdam: Elsevier.
- Roos, Y. H. (1995). *Phase transitions in foods*. San Diego: Academic.
- Roques, M. A. (2005). Conference report of the 14th International Drying Symposium (IDS 2004). *Drying Technology*, 23(1 & 2), 407–411.
- Systat (1990) *Systat 5.02* for Windows, Systat, Inc., Evanston, IL, USA, 60201.
- Vagenas, G. K., & Marinos-Kouris, D. (1990). An analysis of mass transfer in air-drying of foods. *Drying Technology*, 8, 323–342.
- Wolf, I. D., Labuza, T. P., Olson, W. W., & Schafer, W. (1990). *Drying foods at home. Communication and educational technology services*. USA: University of Minnesota.
- Zogzas, N. P., Maroulis, Z. B., & Marinos-Kouris, D. (1996). Moisture diffusivity data compilation in foodstuffs. *Drying Technology*, 14(10), 2225–2254.